Optimal visuo-tactile integration for velocity discrimination of self-hand movements

M. Chancel, C. Blanchard, Michel Guerraz, A. Montagnini, A. Kavounoudias

Optimal visuo-tactile integration for velocity discrimination of self-hand movements

M. Chancel [1,2], C. Blanchard [3], M. Guerraz [2], A. Montagnini [4*], A. Kavounoudias [1*]

[1] Aix Marseille Université, CNRS, LNIA UMR 7260, FR3C,13331 Marseille, France

[2] Université Savoie Mont Blanc, CNRS, LPNC UMR 5105, F-73000 Chambéry, France

[3] University of Nottingham, School of Psychology, NG7 2RD Nottingham, UK

[4] Aix Marseille Université, CNRS, INT UMR 7289, 13385 Marseille, France

* A.M. and A.K. contributed equally to this work.

Corresponding author

Dr. Anne Kavounoudias
Aix-Marseille Université - CNRS
Laboratoire de Neuroscience Intégrative & Adaptative (UMR7260)
3 Place Victor Hugo - 13003 Marseille – France
Phone : +33 413 550 836
Fax : +33 413 550 844
e-mail : Anne.Kavounoudias@univ-amu.fr

Running Head: Optimal visuo-tactile integration in kinesthesia

Abstract

Illusory hand movements can be elicited by a textured disk or a visual pattern rotating under one's hand, while proprioceptive inputs convey immobility information (Blanchard et al., 2013). Here we investigated whether visuo-tactile integration can optimize velocity discrimination of illusory hand movements in line with Bayesian predictions. We induced illusory movements in fifteen volunteers by visual and/or tactile stimulation, delivered at six angular velocities. The participants had to compare hand illusion velocities with a 5°/s hand reference movement in an alternative forced choice paradigm. Results showed that the discrimination threshold decreased in visuo-tactile condition compared to unimodal (visual or tactile) conditions, reflecting better bimodal discrimination. The perceptual strength (gain) of the illusions also increased: the stimulation required to give rise to a 5°/s illusory movement was slower in the visuo-tactile condition compared to each of the two unimodal conditions. The Maximum Likelihood Estimation model satisfactorily predicted the improved discrimination threshold, but not the increase in gain. When we added a zero-centered Prior, reflecting immobility information, the Bayesian model did actually predict the gain increase, but systematically overestimated it. Interestingly, the predicted gains better fit the visuo-tactile performances when a proprioceptive *noise* was generated by co-vibrating antagonist wrist muscles. These findings show that kinesthetic information of visual and tactile origins is optimally integrated to improve velocity discrimination of self-hand movements. However, a Bayesian model alone could not fully describe the illusory phenomenon pointing to the crucial importance of the omnipresent muscle proprioceptive cues with respect to other sensory cues for kinesthesia.

Key-words: Illusions, Bayesian modeling, Kinesthesia, Multisensory integration, Muscle proprioception

New & Noteworthy

The present study demonstrates for the first time that kinesthetic information of visual and tactile origins are optimally integrated (Bayesian modeling) to improve velocity discrimination for self-hand movement. We used an original paradigm consisting in similar illusory hand movements induced through visual and tactile stimulation. By testing the role of other sources of information favoring non-moving hand perception we also highlight the key contribution of the omnipresent muscle proprioceptive information and its over-weighting for kinesthesia.

Introduction

To perceive our body movement in space, we can rely on several sensory inputs. Among them, the involvement of muscle proprioception in kinesthesia has been widely investigated (for reviews see McClosckey, 1978; Roll et al., 1990; Proske and Gandevia, 2012). The visual system also contributes to the sense of movement, as evidenced by vection phenomenon, i.e. a kinesthetic percept elicited by a visual moving scene scrolling in front of a participant (Brandt and Dichgans, 1972; Guerraz and Bronstein, 2008) or under one's limb (Blanchard et al., 2013). Touch, like vision, also conveys kinesthetic information with cutaneous receptors sensitive to the velocity of superficial brushing applied to their receptive fields (Breugnot et al., 2006). Illusions of self-body movements can thus be induced using a tactile stimulus rotating under the palm of the hand (Blanchard et al., 2011, 2013).

However, less is known about how these two sensory modalities interact to estimate self-body motion. Many studies highlighted a perceptual benefit when two or more sensory signals are combined, provided they are temporally and spatially congruent. Based on a probabilistic representation of information and on the assumption that minimizing the variance of the combined perceptual estimate is a primary goal of multisensory integration, the Optimal Cue Combination framework has provided an efficient approach to predict the perceptual enhancement due to

multisensory integration (Landy et al., 2011). In particular, the Maximum Likelihood Estimation (MLE) principle postulates that the multisensory estimate of an event is given by the reliability-weighted average of each single-cue estimates (where reliability is defined as the inverse of variance). MLE predictions have been successfully reported for several multisensory tasks, but mainly when the object of perception is external to the body (Ernst and Banks, 2002; Alais and Burr, 2004; Wozny et al., 2008; Gingras et al., 2009; Gori et al., 2011). Whether Bayesian rules can account for multisensory integration subserving self-body perception has been less investigated, especially with regard to the integration of visuo-tactile kinesthetic cues. Visual and vestibular information were found to be close-to-optimally integrated in the perception of whole-body displacements (Fetsch et al., 2009; Vidal and Bülthoff, 2009; Prsa et al., 2012); as vision and proprioception when evaluating arm movements (Reuschel et al., 2009), positions in space (VanBeers et al., 2002; Tagliabue and McIntyre, 2013), as well as when performing pointing motor tasks (Sober and Sabes, 2003, 2005).

The present study aimed at further investigating whether visual and tactile signals are optimally integrated when estimating self-hand movements. During natural movements, muscle proprioceptive afferents are continuously activated and they cannot be selectively removed without impairing concomitant cutaneous afferents (for instance, an ischemic block affects all large somatosensory fibers, including both cutaneous and proprioceptive fibers (Diener et al., 1984). Therefore, it is usually impossible to estimate the kinesthetic contribution of visuo-tactile modalities independently from muscle proprioception. For this reason, we induced illusory movements rather than actual movements using a visual and/or tactile moving background rotating under the hand, i.e. the participants felt that their hand was passively rotated though it remained perfectly still. We estimated the perceptual benefit of visuo-tactile stimulation compared to each unimodal stimulation in a discriminative test of self-hand movement velocity, and then compared it to the MLE predictions.

However, in our experiment, participants were aware that their hand was not actually moving, and this cognitive component was further strengthened by a proprioceptive feedback from the wrist muscles conveying static information. This Prior knowledge combined with static muscle

4

proprioceptive cues might explain why the perceived velocity of the illusory movements was about six times less than the actual velocity of the stimulation (Blanchard et al. 2013). In the Bayesian framework, sensory illusions have been successfully explained as the result of an optimal combination between noisy sensory information and stimulus-independent Prior knowledge. For example, a Prior favoring low-speed motion can account for several visual illusory phenomena observed in motion vision (Weiss et al., 2002; Montagnini et al., 2007). Studies about self-body perception used a Gaussian low-speed Prior distribution to account for top-down expectations that influence perceptual performance (Jürgens and Becker, 2006; Laurens and Droulez, 2006; Dokka et al., 2010; Clemens et al., 2011).

Therefore we tested a Bayesian model including a Gaussian Prior distribution, as well as a proprioceptive Likelihood, both centered on zero, in order to account for the strong belief in favor of immobility and for the omnipresent static information from muscle spindle endings. The combination of these two Gaussian distributions centered on zero should provide a theoretical ground for the very low gain of the illusory hand-motion perception. For the sake of simplicity, we will refer to this combined information as zero-centered Prior. We also manipulated this Prior static information by disturbing proprioceptive feedback. To this end, we equally applied a co-vibration onto the participants' antagonist wrist muscles (*Noisy* condition). We expected to make the muscle proprioceptive inputs less reliable, and consequently to lower the weight of the static information taken into account in the Prior distribution and to increase the gain of illusory perception.

Method

Participants

Twenty right-handed volunteers (14 women) with no history of neurological disease agreed to participate to this study. They all gave their informed consent, conforming to the Helsinki declaration,

and the experiment was approved by the local Ethics Committee (CCP Marseille Sud 1 #RCB 2010-A00359-30). Five of them did not experience any illusory perception during the tactile stimulation and were therefore not included in the complete series of experiments and analysis.

Stimuli (Fig. 1)

Tactile stimulation was delivered by a motorized disk (40 cm in diameter) covered with cotton twill (8.5 ribs/cm), which is a material known to efficiently activate cutaneous receptors (Breugnot et al., 2006). The disk rotated under the participant's right hand in a counterclockwise direction with a constant angular velocity ranging from 10 to 45 °/s (Fig. 1B). Visual stimulation consisted of a projection of a black and white pattern on the disk. To give the participant the feeling that the pattern was moving in the background, i.e. under his/her hand, a black mask adjusted to the size of each participant's hand was included in the video and prevented the pattern from being projected onto his/her hand. The pattern was rotating around the participant's right hand with a constant counterclockwise angular velocity ranging from 10 to 45 °/s (Fig. 1C). These two types of stimulation were delivered for six seconds either separately (unimodal conditions) or simultaneously (bimodal condition) at six different velocities (10, 20, 25, 30, 35, and 45 °/s). These stimulation velocities were chosen based on a previous study (Blanchard et al., 2013) to induce efficient illusory movements with a perceived velocity well distributed around 5 °/s (reference velocity). In the *Noisy* conditions, muscle proprioception was disturbed using low amplitude mechanical vibration (0.5 mm peak-to-peak) set at a constant low frequency (20 Hz). We used two vibrators each made of a biaxial DC motor with eccentric masses forming a 5-cm long and 2-cm in diameter cylinder. As shown on Figure 1D, they were fixed on both sides of the participant's right wrist to stimulate equally and simultaneously two antagonist muscle groups: the *longus pollicis* and the *extensor carpi ulnaris* muscles. Indeed, microneurographic studies showed that such low amplitude vibration preferentially activates muscle spindle primary endings. Roll et al (1989) have shown that in 10 to 100

153 Hz vibration range, primary muscle spindle endings respond with a frequency of discharge equal to the

154 vibration frequency (with a 1 : 1 mode of response), resulting in a masking effect of spontaneous

155 natural discharges, usually ranged between 3 to 15 Hz in the absence of vibratory stimulation (Roll et

156 al., 1989). When applied onto a single muscle group, vibration stimulation can elicit an illusory

157 sensation of limb movement but any illusion is cancelled when a concomitant vibration is equally

158 applied onto antagonist muscles (Calvin-Figuière et al., 1999). Therefore, by equally co-stimulating

159 wrist antagonist muscles, we expected to disturb proprioceptive afferents without inducing any illusory

160 sensation of movement. The stimuli were delivered using a National Instruments card (NI PCI-6229)

161 and a specifically designed software implemented in LabView (V.2010).

162

163   ***Insert Figure 1 around here***

164

165 ***Procedure***

166   Participants sat on an adjustable chair in front of a fixed table with arm-rests immobilizing their

167 forearms, their left hand resting on the table and their right hand on the motorized disk. A small

168 abutment in the disk center placed between their index and middle finger kept their hand from moving

169 with the disk when it rotated. Head movements were limited thanks to a chin- and chest-rest allowing

170 participants to relax and sit comfortably. The experiment took place in the dark and participants wore

171 headphones to block external noise, as well as shutter glasses partially occluding their visual field and

172 reducing it to the disk surface only.

173 *Training phase*

174   Before the experimental session, each participant underwent two training sessions. First, a 15

175 minute session consisted of 150 trials of separate tactile and visual stimulation applied at medium

176 velocity (25 °/s). To be included in the experiment, the participants had to feel illusory hand rotations

177 in at least 80 % of the trials.

178   Then, the participants were trained to perform a reproducible 5 °/s clockwise hand rotation. During this

179   second 15 minute session, with their middle fingers they had to follow a red line moving at 5 °/s that

180   was repeatedly projected onto the disk every 7.5 seconds. Participants were asked to memorize the

181   movement using all the available information (tactile, visual and proprioceptive feedback, plus efferent

182   motor command). This 5 °/s movement was chosen as the reference to which participants would have

183   to compare their perception during the discrimination test phase.

184

185

186   *Discrimination test phase*

187   The experimental test consisted of a 2-AFC (alternative forced choice) discrimination

188   task with constant stimuli. A stimulation condition (visual, tactile or combined) and the

189   reference movement were presented by pairs in random order. The participants were instructed

190   to say out loud whether the illusory movement they perceived was faster or slower than the

191   reference movement.

192   The reference movement executed during the experimental test was similar to that performed

193   during the training phase except that the red line appeared only during the first and the last of the 6

194   seconds of the movement duration to prevent the participants from using only visual feedback.

195   Three stimulation conditions were randomly intermixed within the experimental sessions: two

196   unimodal conditions (tactile T, visual V) and one bimodal condition (visuo-tactile VT). For each

197   stimulation condition, 6 intensities were tested and presented immediately before or after the reference

198   movement. All stimuli lasted 6 seconds (as the reference movement) and the inter-stimulus intervals

199   ranged between 1.7 and 2.3 seconds. Before each reference/stimulation pair, a white line was projected

200   to make sure that participants always positioned their hand in the same orientation. Participants were

201   instructed to focus on their hand to estimate as accurately as possible whether the illusory movement

202   they perceived was faster or slower than the reference movement they executed just before or just after

203   each stimulus. They had to keep their eyes open, except if a green screen appeared signaling them to

8

close their eyes before a tactile-only stimulus. At the end of each pair (reference/stimulation) presentation, participants had 2 seconds to answer ("*faster*" or "*slower*") and 3 seconds (± 300 ms) before a new pair was presented. The presentation order of the 18 stimulation conditions was counterbalanced for each subject.

During the *Standard* condition test, participants were asked to compare 270 reference/stimulation pairs (3 conditions * 6 intensities * 15 trials) divided into four sessions of 10 minutes each performed on two different days (at the same time during the day). Thirteen of the fifteen participants were tested in four additional *Noisy* condition sessions of 10 minutes during which the same block of 270 pairs of reference/stimulation was presented while participants underwent co-vibrations of their antagonist wrist muscles.

Movement acquisition and kinematic analysis

Participants were asked to compare the velocity of each illusory movement they experienced during the unimodal and bimodal stimulation conditions with the velocity of the same reference movement, consisting of a clockwise rotation of the right hand at 5 °/s that they actively performed just before or just after every stimulus. All reference movements were recorded using an optical motion capture system (CODAmotion, Charnwood Dynamics, Rothley, UK) composed of 3 infrared 'active' markers and one camera to track the 3D marker positions (sampling frequency: 10 Hz). Markers were attached to the participants' middle finger, on the top of their hand back, and on the last third of their forearm to capture the angular rotation of their wrist during the reference movement execution. For each participant, the mean angular velocity of hand movements was extracted with the Codamotion Analysis software (V6.78.2). Reproducibility of the reference movement across the 270 trials during the *Standard* experiment was further tested by a one-way ANOVA for each participant with the session (4 sessions) as experimental factor for the *Standard* condition (without vibration) and the *Noisy* condition (with co-vibration stimulation). As expected, no significant difference in the mean velocity of the reference movement was found between sessions whatever the participant neither in the

230   *Standard* nor the *Noisy* condition. Note that individual variability estimated from the four sessions

231   ranged between 0.22 and 0.37 °/s. We further verified the precision of estimation of the reference

232   movement in a complementary experiment performed on ten naïve participants consisting in a

233   discrimination task between several self-hand rotations actively executed. Participants were asked to

234   compare the velocity of the fixed reference movement set at 5°/s (like in the main experiments) with 8

235   other hand movement velocities (3.5°/s, 4 °/s, 4.5 °/s, 4.75 °/s, 5.25 °/s, 5.5 °/s, 6 °/s, or 6.5 °/s). Again,

236   the estimated variability was found to be small (ranging from 0.33 to 0.79 °/s).

237   A one-way ANOVA was also performed to ensure that reference movement was not

238   significantly different between participants (*Standard* condition: $F_{(3, 42)} = 1.05$, $P = .38$; Noisy

239   condition: $F_{(3, 36)} = 0.21$, $P = .89$). Finally, a Student's paired *t* test was used to ensure the

240   reproducibility of the reference movement between the *Standard* condition and the *Noisy* condition.

241   There was no significant difference between these conditions (mean$_{Standard}$ = 4.6 ± 0.08 °/s mean$_{Noisy}$ =

242   4.7 ± 0.07 °/s; $P = .34$), suggesting that participants referred on average to the same velocity of

243   reference movement in both conditions.

244   *Data analysis*

245   In order to evaluate and compare participants' perceptual performance across the three

246   stimulation conditions (T, V, VT), the psychometric data (i.e. the proportion of "faster than the

247   reference" answers at different stimulation intensities) were fitted by a cumulative Gaussian function:

248   $$P(x) = \lambda + (1 - 2\lambda)\frac{1}{\sigma_\psi\sqrt{2\pi}}\int_{-\infty}^{x} e^{-\frac{(y-\mu_\psi)^2}{2\sigma_\psi^2}}\, dy$$

249   where x represents the stimulus velocity (in degrees per second); μ_ψ is the mean of the Gaussian, i.e.

250   the Point of Subjective Equality (PSE) that corresponds to the stimulation intensity leading the

251   participant to perceive an illusory movement on average as fast as the reference set at 5 °/s; σ_ψ is the

252   standard deviation of the curve, or discrimination threshold, which is inversely related to the

253   participant's discrimination sensitivity. In other words, a smaller σ_ψ value corresponds to a higher

254   sensitivity in the discrimination task. The two indices, PSE and σ_ψ, characterize the participant's

performance. λ accounts for stimulus-independent errors due to participant's lapses and was restricted to small values ($0 < \lambda < 0.06$, Wichmann and Hill, 2001), This parameter is not informative about the perceptual decision, thus we disregarded it for the following analyses. Psignifit toolbox implemented on Matlab software (© 1994-2014 The MathWorks, Inc.) was used to fit the psychometric curves (Wichmann and Hill, 2001).

To compare discrimination sensitivity across the three stimulation conditions (T, V and VT), we performed a one-way repeated-measures ANOVA with Tukey post-hoc tests on σ_ψ values. In addition, for each participant, the enhancement of the visuo-tactile discrimination sensitivity over the best unisensory one was assessed using the multisensory index (MSI) as defined by (Stein et al., 2009). Since an improvement of discrimination sensitivity corresponded to a decrease in σ value, the MSI was computed as follows:

$$MSI\,(\sigma_\psi) = \frac{Min(\sigma_{\psi T}; \sigma_{\psi V}) - \sigma_{\psi VT}}{Min(\sigma_{\psi T}; \sigma_{\psi V})}$$

To quantify the perceptual strength of the illusions, the gain of the responses in the different stimulation conditions was assessed as follow (in percentage):

$$Gain = \frac{Vref}{PSE} * 100$$

with the reference velocity V_{ref} set at 5 °/s.

For the fifteen participants, we compared the response gains between the three sensory stimuli (T, V and VT) using a one-way repeated-measure ANOVA with Tukey post-hoc tests. For the thirteen participants that underwent the *Noisy* condition, a two-way repeated-measure ANOVA was also performed on the illusion gains to test the effect of the sensory stimulation (T, V and VT) and the experimental condition (*Standard* vs *Noisy*).

The enhancement or depression of the visuo-tactile response gain over the best unisensory response gain was computed using the multisensory index (MSI) as defined by (Stein et al., 2009)

$$MSI\ (Gain) = \frac{Gain_{VT} - Max(Gain_T; Gain_V)}{Gain_{VT}} * 100$$

Models

The Maximum Likelihood Estimate model used to predict optimal multimodal discrimination performance

Insert Figure 2 around here

As illustrated in Figure 2, the minimum-variance linear combination model (often referred to as Maximum Likelihood Estimate (MLE) model) predicts how an "optimal observer" would combine two unbiased sensory signals to optimize the resulting perception (in the sense of minimizing its variance) relative to the two unimodal representations. According to MLE rules (which are just one particular instantiation of the more general Bayesian framework, see Landy et al. 2011), the optimal perceptual estimate in visuo-tactile stimulation can be described by the normalized product of the unimodal Likelihood distributions $P(\vartheta_T | \vartheta)$ and $P(\vartheta_V | \vartheta)$, with the underlying assumption that visual and tactile sources are conditionally independent variables affected by Gaussian noise:

(1) $\qquad\qquad P(\vartheta_{VT} | \vartheta) \propto P(\vartheta_T | \vartheta) * P(\vartheta_V | \vartheta)$

where ϑ_T, ϑ_V and ϑ_{VT} are the tactile, visual and visuo-tactile estimates of hand velocity for a given value of stimulation velocity ϑ.

The visuo-tactile Likelihood resulting from the normalized multiplication of the two unimodal Gaussians is a Gaussian distribution itself, with a variance $\sigma^2{}_{VT}$ related to the unimodal variances through the following equation

(2) $\qquad\qquad \frac{1}{\sigma^2{}_{VT}} = \frac{1}{\sigma^2{}_V} + \frac{1}{\sigma^2{}_T}$

12

303 Therefore, equation 2 implies that if the two sensory signals are optimally integrated, the visuo-tactile

304 variance is smaller than the variance of either modality in isolation, thus leading to a sensitivity

305 enhancement.

306 The MLE model and its predictions can easily be tested on the behavioral data of a multisensory

307 discrimination experiment. It can be shown that the same relation presented in equation 2 for the

308 variance of the sensory likelihood does actually apply to the standard deviation (σ_ψ) of the estimated

309 cumulative-Gaussian psychometric curve (i.e. its discrimination threshold). In particular, in this study,

310 predicted and observed visuo-tactile discrimination thresholds were compared in order to determine if

311 the integration of vision and touch was optimal with regard to the discriminative sensitivity of the

312 participants.

313 It should be noticed that in the present experimental context, the uncertainty related to the reference

314 movement velocity estimation could account for a portion of the estimated discrimination threshold σ_ψ.

315 We will address this issue in the next session.

316

317 *A Bayesian model to account for the low-perceptual gain of movement illusions*

318   In the present study, kinesthetic illusions of hand movements were induced while participants were

319 aware that their hand was actually not moving. This Prior knowledge was also supported by muscle

320 proprioceptive feedback from their stationary wrist. The conflict between this static information and

321 the moving tactile or visual information may account for the extremely low gain of the velocity

322 illusions with respect to the actual velocity of the moving stimuli (Blanchard et al., 2013).

323   In order to account for the low gain of the uni- and multimodal illusions, a more complex Bayesian

324 model was elaborated including a zero-centered Gaussian Likelihood accounting for muscle

325 proprioceptive cues and a Gaussian Prior distribution centered on zero too. The combination of those

326 two distributions is also a zero-centered Gaussian distribution. Therefore, to preserve the model

327 parsimony, we will treat these distinct contributions as a single probability distribution and we will

328 refer to it as "Prior" throughout the present manuscript.

329   The sensory Likelihood and the Prior distributions are combined according to Bayes' rule to obtain

330   the Posterior distribution:

331    $\qquad$ (3) $\qquad$ $P(\vartheta|\vartheta_i) \propto P(\vartheta_i|\vartheta) * P(\vartheta)$

332   with $P(\vartheta)$ = Prior probability distribution of hand velocity, $P(\vartheta_i|\vartheta)$ = sensory Likelihood for the

333   modality i, and i = T,V or VT.

334   The parameters (mean and variance) of the Bayesian Gaussian distributions are linked by the

335   following relations:

336    $\qquad$ (4)
$$\frac{\mu_{Post_i}}{\sigma^2_{Post_i}} = \frac{\mu_i}{\sigma^2_i} + \frac{\mu_{prior}}{\sigma^2_{Prior}}$$

337

338
$$\frac{1}{\sigma^2_{Post_i}} = \frac{1}{\sigma^2_i} + \frac{1}{\sigma^2_{Prior}}$$

339   with i = T, V or VT, μ_{Prior} = 0 °/s, σ^2_{Prior} is the unknown variance of the Prior (assumed to be constant

340   throughout the different experimental conditions), μ_i the mean of the Likelihood, σ^2_i the unknown

341   variance of the Likelihood and, similarly, μ_{Post_i} and $\sigma^2_{Post_i}$ are the mean and variance of the Posterior

342   distribution. In line with most Bayesian models, we assumed that the Likelihood mean exactly matches

343   the velocity stimulation ($\mu_i = \vartheta_i$) as it represents the first stage of (presumably unbiased) sensory

344   encoding of global motion information. We also assumed that σ^2_i does not depend on velocity in the

345   considered range. Although this last assumption is probably not true in general (e.g. Stocker &

346   Simoncelli 2006), it seems to be a reasonable approximation for the relatively small range of

347   stimulation velocities considered here.

348   Given all the above-mentioned assumptions, the estimated parameters of the psychometric function

349   can be put in relation to the parameters of the hidden Bayesian distributions. A Bayesian ideal observer

350   uses the information provided by the Posterior distribution to formulate a perceptual judgment, such as

351   the velocity discrimination in our study. As shown in Figure 3, the proportion of judgments of the type

352 "*test faster than reference*" is equal to the integral of the Posterior distribution over the interval

353 $]V_{ref}: +\infty[$

354

355

356 Let us consider two values of the stimulation velocity that correspond to the critical parameters of the

357 psychometric curve, namely the PSE and the value at which $\Psi = 0.84$ which corresponds by

358 definition to (PSE+σ_Ψ).

359 When the test velocity $\vartheta_i = PSE$ the ideal observer perceives on average by definition a velocity

360 equivalent to the reference velocity V_{ref}. Thus the mean (and most likely value) of the Posterior

361 distribution μ_{Post} is equal to V_{ref}.

362 On the other hand, when the test velocity is $\vartheta_i = PSE + \sigma_\Psi$, the integral under the Posterior is 0.84,

363 which - on the ground of the assumption of normality - implies that its mean μ_{Post} is equal to ($V_{ref} +$

364 σ_{post}).

365 By substituting these equalities in the system of equations 4, we obtained the expression of the

366 variance of the three Bayesian distributions as a function of the parameters of the psychometric curve

367 (PSE$_i$, σ_i) and of V_{ref}.

368 (5)
$$\frac{1}{\sigma^2_i} = \frac{PSE_i}{V_{ref}} * \frac{1}{\sigma^2_{\Psi i}}$$

369

370 (6)
$$\frac{1}{\sigma^2_{Prior}} = \frac{PSE_i}{V_{ref}} * \frac{1}{\sigma^2_{\Psi i}} * (\frac{PSE_i}{V_{ref}} - 1)$$

371

372 (7)
$$\frac{1}{\sigma^2_{Post}} = \frac{PSE_i{}^2}{V_{ref}{}^2} * \frac{1}{\sigma^2_{\Psi i}}$$

373

Note that these equations hold for each type of stimulation (T, V or VT). The variance of the Prior distribution was thus estimated (through Equation 6) for each of the unimodal conditions V and T. Consistent with our assumption of a constant Gaussian Prior noise across experimental conditions, we verified that the σ_{Prior} estimated by the "tactile" and the "visual" equation (6) did not differ significantly (Student's paired t-test: $P = .063$). We used the mean of the Prior variance estimated from the visual and tactile psychometric parameters (Equation 6) for the later steps (see also Fig. 4; Step 1). We then applied the MLE predictions for the estimate of the Likelihood variance in the condition of visuo-tactile stimulation (Equation 2) and then inverted the Equations 5, 6 and 7, relating the Bayesian to the psychometric parameters, in order to predict the bimodal point of subjective equality PSE_{VT} (Fig. 4; Step 2),

$$(8) \qquad PSE_{VT}^{pred} = V_{ref} \; * \; \left(1 + \frac{\sigma^2_{VT}}{\sigma^2_{Prior}}\right)$$

where both σ^2_{VT} and σ^2_{Prior} can be expressed as functions of the unimodal psychometric parameters. For all participants, the predicted gain G_{VT} of the visuo-tactile illusion in the *Standard* condition could finally be compared to the observed visuo-tactile gain.

As previously pointed out, the uncertainty related to the estimation of the reference movement velocity could account for a portion of the perceptual variability in our hand-velocity discrimination task, whatever the sensory stimulation. Therefore we assessed its influence by including the individual variability of the reference movement reproduction (see Methods section) in the estimation of the global uncertainty for the velocity discrimination task. However, doing so increased the complexity of the model without improving the predictions, nor changing the core results. For the sake of parsimony, we will only briefly present the impact of this additional component of perceptual uncertainty on the predictions at the end of the Result section.

In addition, the same analysis was performed on perceptual responses elicited in the *Noisy* condition, where co-vibration was applied onto antagonist wrist muscles to disturb static muscle

399   proprioceptive feedback. The variance of the Prior σ^2_{Prior} in the *Noisy* condition was estimated and the

400   visuo-tactile illusion gain G_{VT} was predicted.

401   The relative contribution of the Prior in the final perception was also assessed by computing the

402   relative weight of the Prior with respect to the visual and tactile weights, as follows:

403 $$\omega_{Prior} = \frac{\sigma^{-2}_{Prior}}{\sigma^{-2}_{Prior} + \sigma^{-2}_{T} + \sigma^{-2}_{V}}$$

404

405   The relative weights of the Prior obtained in *Standard* and *Noisy* conditions were compared using a

406   Student's paired t-test.

407   Finally, to test whether the model better fit the visuo-tactile performances in the *Noisy* condition

408   compared to the *Standard* condition, the differences between predicted and observed gains in the two

409   conditions were compared using a Student's paired t-test.

410   ***Insert Figure 4 around here***

411

412 ## Results

413

414 ***Discriminative ability for hand movement velocity based on visual and/or tactile inputs***

415   As expected, for all the participants included in the study, the counterclockwise rotation of the

416   visual and/or tactile stimulation gave rise to an illusory sensation of rotation of their stimulated hand,

417   which was always oriented in the opposite direction, i.e. clockwise. For each stimulation condition (T,

418   V, VT) randomly applied at six different velocities, participants reported whether the illusion was

419   faster or slower than the 5 °/s clockwise reference rotation they actively performed just before or just

420   after the stimulation delivery. To compare the participants' performance in the velocity discrimination

421   task between tactile, visual, and visuo-tactile stimulation, the probability of perceiving the illusion as

422   faster than the reference movement was fitted by a cumulative Gaussian function for the tested

423   stimulus velocities to obtain three individual psychometric curves.

As shown in the example of Figure 5A, the participant experienced an illusory movement with a velocity close to the 5 °/s reference when the tactile or the visual stimulation was rotating around 29.8 °/s and 28.8 °/s, respectively. The participant's ability to discriminate the velocity of his/her hand movement improved in the visuo-tactile condition compared to the unimodal ones, as attested by an increased slope of the visuo-tactile psychometric curve. More precisely, the discrimination threshold σ (i.e. the increase in stimulation velocity required to induce an illusory movement faster than the reference movement in 84 % of the trials with respect to 50 % of the trials) was lower in the visuo-tactile condition (mean σ_{VT} = 6.02 ± 2.19 °/s) than in the unimodal conditions (mean σ_T = 8.67 ± 3.6 °/s; mean σ_V = 7.68 ± 3.5 °/s). In other words, the decrease in σ value reflected the fact that the velocity discrimination ability of this participant increased in the visuo-tactile condition.

These individual results were confirmed at the group level (Fig. 5B). Performances in velocity discrimination changed according to the stimulation condition ($F_{(2, 28)}$ = 12.375, P = .00014). The mean σ decreased significantly in the visuo-tactile condition in comparison with the tactile (post-hoc test: P < .001) and visual conditions (post-hoc test: P = .0025). Discrimination thresholds for the velocity discrimination task did not significantly differ between the two unimodal conditions (P = .58).

In order to quantify the benefit resulting from visuo-tactile stimulation, the multisensory index (MSI) was calculated individually for the σ values. This index, expressed in percentage, reveals for each participant the enhancement (or depression) of the multisensory sensitivity over the best unisensory response (Stein et al., 2009). For eleven of the thirteen participants, the multisensory response showed a positive benefit on the discriminative threshold σ. Quantitatively, the visuo-tactile σ values for those eleven participants were lower than the lowest of the unimodal σ, with an MSI ranging between 3 % and 40 % (Fig. 5C). Only two among 15 participants did not show an improvement of their discriminative sensibility in the visuo-tactile condition.

447

As depicted in Figure 2, the MLE model predicts an improved discrimination performance in the multimodal condition. The MLE-predicted visuo-tactile σ values were estimated for each participant on the basis of his/her performances in the two unimodal conditions. As illustrated in Figure 5D, comparing these estimates to the experimental observations during the visuo-tactile condition showed that the data estimates did not differ significantly from the observed σ values (Student's Paired t test, P = .55). Note that including the variability of the reference reproduction task in the model did not change the predictions of the discriminative thresholds in any appreciable way (0.9 % of difference in the worst case…).

<center>***Insert Figure 5 around here***</center>

A low-perceptual gain for movement illusions

Standard condition

In the individual results presented in Figure 6A, illusory movement was perceived at a velocity close to the 5 °/s reference when the tactile or the visual stimulation was rotating at about 29 °/s, with a point of subjective equality (PSE) estimated at 28.8 and 29.8 °/s, respectively. When the two kinds of stimulation were combined, the velocity of the stimulation required to evoke an illusion close to the 5 °/s reference dropped to 20.5 °/s (Fig. 6A). The decrease in PSE reflected the fact that the participant perceived a faster illusory movement with combined visual and tactile stimulation compared to only one kind of stimulation. These results can also be expressed in terms of response gain, classically defined as the ratio between the perceived illusion velocity and the actual velocity of the stimulus (see Method section). A value of 100 % would indicate that the participant perceived a hand movement at the same velocity as the actual stimulation velocity. In our experimental paradigm, the gains of the illusions were always much lower than 100 %. They were on average about 19.9 % (± 2.7 % SD) and 18.4 % (± 2.9 % SD) for the tactile and visual stimulation, respectively. During visuo-tactile

stimulation, the gain significantly increased, up to 23.7 % (± 3.5 % SD) in comparison with unimodal

tactile (post-hoc test: P = .0004) and visual (post-hoc test: P < .0001) stimulations: illusion velocity got

closer to the actual stimulation velocity in visuo-tactile condition (Fig. 6B). A more detailed analysis

showed that the multimodal gain increased for all participants except one (Fig. 6C). This increase was

also attested by positive MSI values, ranging from 1 % to 40 % for 14 of the 15 participants (mean

MSI = 14 % ± 13).

Insert Figure 6 around here

To account for these low-perceptual gains, we then considered a more complex model than the MLE,

including the influence of the "non-moving hand information" *a priori* present in our experimental

paradigm. Indeed, in addition to the omnipresent proprioceptive static cue, participants were always

aware that their hands were not actually moving. By modeling the "non-moving hand information" as

a Gaussian distribution centered on zero, the variance of this Prior was first estimated through the

observed data obtained in the two unimodal conditions (Fig. 3 & 4 Step 1). In line with our assumption

that the Prior distribution should be constant over the various sensory conditions, we found that the

variance estimates based on each single sensory performance did not differ significantly (P = .18).

The visuo-tactile Likelihood was then predicted by combining the estimated Prior distribution with the

estimated unisensory Likelihoods (see Fig. 3 & 4 Step 2).

This model predicted that the gain of the illusion in the visuo-tactile condition would improve

compared to the unimodal ones. However, the observed increase in gain was less than that predicted by

the model (Fig. 6D). By taking into account the variability of the reference movement perception in the

model, predictions were not improved (they became actually worse, in the worst case, discrepancies

between observations and predictions of the gain went from 3.9 % to 9.8 %), but the discrepancy

between data and model predictions did not qualitatively change, highlighting in all cases an

overestimation of the gain increase by the Bayesian complete model.

Noisy condition

499   To further explore the influence of the "non-moving hand" cues in our paradigm, the same

500   experiment was performed while muscle proprioception was disturbed by equivalent vibrations applied

501   on antagonist wrist muscles involved in left-right hand movement: the right *pollicis longus* and *carpi*

502   *ulnaris extensor* muscles. Applied on antagonist muscles with the same low frequency, mechanical

503   vibration equally activates muscle spindle endings, masking natural muscle spindle afferents without

504   giving rise to any relevant movement information (Roll et al., 1989; Calvin-Figuière et al., 1999).

505   Before the beginning of each experimental session, we ensured that muscle co-vibration did not induce

506   any movement sensation.

507   During co-vibration, all the participants were still able to experience the illusory movement

508   elicited by the tactile and/or visual stimulation. In the *Noisy* condition, the stimulus velocity required

509   for the illusory movement to reach a velocity close to the reference value was lower than that

510   previously observed in the *Standard* condition where no vibration was applied. A two-way ANOVA

511   analysis showed that the gains of the perceptual illusions increased significantly in the *Noisy*

512   conditions compared to the *Standard* ones (Main effect of condition ($F_{(1, 12)} = 26.003$; $P = .00026$).

513   When the two *Noisy* and *Standard* conditions were confounded, the gain observed in the visuo-tactile

514   conditions was significantly higher than those observed in the tactile and visual conditions ($F_{(2, 24)} =$

515   25.37; $P < .0001$) (Fig.7). No significant interactions were found between the condition (*Noisy* vs

516   S*tandard*) and stimulation (T, V, VT) factors.

517

518   ***Insert Figure 7 around here***

519

520   As in the previous *Standard* experiment, we estimated the variance of the Prior based on unimodal

521   responses collected during co-vibration. With degraded muscle proprioceptive information, the

522   influence of the "non moving hand" information modeled by the Prior was supposed to be reduced in

523   the *Noisy* conditions. As expected, for the 13 participants tested, the relative weight of the Prior

524 (compared to the tactile and visual relative weight) was lower in the *Noisy* experiment (0.89 ± 0.03)

525 than in the *Standard* one (0.95 ± 0.017; Student's paired *t* test: *P* = .011).

526 In addition, the predicted gains of the visuo-tactile responses were estimated on the basis of the

527 unimodal and Prior distributions obtained with concomitant co-vibration. Although the predicted gains

528 were still higher than those observed experimentally, the discrepancy between data and model

529 predictions was reduced in the *Noisy* experiment with respect to the *Standard* one (Student's paired *t*

530 test: *P* = .019; see Figure 8).

531 ***Insert Figure 8 around here***

532

Discussion

533 **Discussion**

534 ***Optimal visuo-tactile integration in velocity discrimination of self-hand movements***

535 The present study shows that visual and tactile motion cues can be equivalently used by the

536 CNS (central nervous system) to discriminate the velocity of self-hand movements. By combining both

537 types of stimulation at the same velocity, one can assume that we generated congruent multisensory

538 signals, as during actual hand movements. As expected, we observed a multimodal benefit provided by

539 the combination of visual and tactile motion cues when participants evaluated the velocity of self-hand

540 illusion rotation. This behavioral improvement was first of all attested by a better discrimination ability

541 (a lower discrimination threshold) in bimodal than in unimodal conditions.

542 The perceptual benefit of combined vision and touch had mainly been estimated when one has

543 to assess properties of an external objet like its size (Ernst and Banks, 2002) or its speed (Bensmaia et

544 al., 2006; Gori et al., 2011). In those studies, as in the present one, the multimodal benefit is well

545 predicted by the MLE principle suggesting that vision and touch are combined in an optimal way when

546 discriminating perceived self-hand velocity.

547 Moreover, participants' ability to discriminate the velocity of an illusory hand movement was

548 equivalent when based on the rotation of either the tactile disk or the visual background with a

22

549 discrimination threshold about 8 °/s for both conditions. This is consistent with the study by Gori et al.

550 (2011) showing equal sensitivities to discriminate the velocity of external motion signals of tactile or

551 visual origin. One can thus hypothesize that common inferential processes take place in situations of

552 visuo-tactile integration in the context of velocity discrimination, whether the perceived object is the

553 self or an external object.

554 *Influence of the non-moving hand Prior in the low-perceptual gain of movement illusions*

555   A strong difference emerges for the absolute estimation of the velocity depending on whether

556 visual and tactile motion signals are related to an external object or to self-body. Whereas velocity

557 estimation of a tactile stream on a fingertip is close to the actual velocity of the moving object

558 (Bensmaia et al., 2006), velocity of the perceived self-hand movement in the present experiment was

559 drastically underestimated with a perceived movement speed always lower than 30 % of the actual

560 visual or tactile stimulation velocity. One plausible explanation is that since proprioceptive afferents

561 from participants' wrist muscles informed the CNS that the hand was not actually moving, the sensory

562 conflict might have resulted in a slower perception of hand rotation. To account for this unavoidable

563 proprioceptive feedback together with the fact that participants knew that their hand was actually not

564 moving, we developed a Bayesian model including a Prior term defined as the product of two

565 Gaussian distributions (the Proprioceptive static sensory Likelihood and the cognitive Prior) centered

566 on zero. We postulated that, when visual or tactile stimulation was applied, the final perception of

567 illusory hand movement resulted from the combination of the visual, tactile or visuo-tactile motion

568 cues with this zero-centered Prior. Our parameter-free Bayesian model successfully predicted a gain

569 increase in visuo-tactile illusions compared to unimodal ones. In the Bayesian framework this effect is

570 explained by the stronger weight of the sensory information when two modalities are optimally

571 combined and hence reliability is increased. In a self-angular displacement estimation task, Jürgens

572 and Becker (2006) had postulated a Prior favoring a particular rotation speed to account for the

573 velocity-dependent bias observed in the participants judgments. Albeit that study did not test a

574 quantitative prediction on the observed bias reduction in multisensory stimulation, the authors'

575 conclusions are consistent with ours and point to a probabilistic integration of sensory representations

576 with a prior knowledge as postulated by Bayes theory. However, the observed gain increase in the

577 present experiment did not match the predicted values, which were over-estimated. In the following

578 section we discuss some possible explanations.

579

580 *Suboptimal multisensory integration: insights into the underlying mechanisms*

581 Deviations from optimal integration predictions have already been reported in cases of sensory

582 conflicts, when sensory information is strongly non-coherent across different modalities. Suboptimal

583 cue weights have been reported in conflictual situations where visual and vestibular inputs are

584 manipulated to give incongruent spatial information relative to passively imposed body rotations (Prsa

585 et al., 2012). In the latter case, participants over-weighted the visual cues to discriminate the angle of

586 imposed rotations. Conversely, vestibular cues were found excessively preponderant to visual cues in a

587 heading perception task (Fetsch et al., 2009).

588 In the present experiment, several explanations may account for the suboptimal benefit on the

589 perceptual gain for visuo-tactile stimulation.

590 First, it has been shown that in case of extreme conflict, integration can be prevented, favoring

591 segregation of the multisensory information (Bresciani et al., 2004; Roach et al., 2006; Körding et al.,

592 2007; van Dam et al., 2014). Accordingly, causal inference models predict a variable degree of

593 multisensory integration according to the probability of the incoming signals to be causally related to a

594 common origin in the world (Körding et al., 2007). In the present study, one can speculate that, if the

595 statistical inference process assigns high weight to a single cause (proprioception, vision and touch all

596 originating from the same true source), then one would indeed find a strengthening of the illusion

597 when a second moving cue is added to the first one. On the other hand, having two moving sensory

598 cues instead of one may increase the conflict between static and movement information, thus leading

599 to a lower weight for the common origin hypothesis. In the latter case, this conflict increase may have

600 degraded multisensory integration and may then have led the participants to partly attribute the visual

601 and tactile motion cues to a different origin, in the environment, rather than their own body. However,

602 a change in causal attribution does not seem to fully explain the present results since it is not consistent

603 with the observation of an increased (although suboptimal) gain in the visuo-tactile condition and also

604 the fact that all the participants reported more salient illusory hand movements in bimodal compared to

605 unimodal conditions. Lastly, segregation is more likely to occur for large discrepancies between cues.

606 Therefore future studies should be conducted to test whether increasing the conflict between static and

607 motion information (using higher velocity stimulation) results in a greater deviation from optimality.

608 Regardless of the conflict between static and motion cues, a second explanation for the

609 overestimation of the bimodal gain improvement can be considered. One can speculate that there is an

610 illusory percept that is being used for a behavioral report and simultaneously a non-reported judgment

611 of background motion and those may interact. In this context, combining visual and tactile cues leads

612 to a decrease in the variability of the velocity estimate, both for self-body movements (as suggested by

613 our psychophysical results) and for external object motions (Gori et al, 2011). As a consequence, if

614 participants have a more coherent percept of the rotation of the environment under their hand, this

615 should in turn facilitate the attribution of the movement to the environment rather than to the hand

616 during the bimodal condition compared to the unimodal conditions, and finally result in sub-optimal

617 performances as compared to Bayesian predictions. Nevertheless, this argument alone fails to explain

618 the observed improvement of gain predictions in the *Noisy* condition. Indeed, muscle proprioceptive

619 noise should not have affected the way external object motion was perceived.

620 Finally, taking into account the crucial role of muscle proprioception in kinesthesia, the

621 suboptimality in the present study can be interpreted as a weighting bias in favor of this modality.

622 Biases toward one sensory cue in multisensory conflicting situations that cannot be explained by a

623 Bayesian weighting process can rather be attributed to a recalibration mechanism (Adams et al., 2001;

624 Block and Bastian, 2011; Wozny and Shams, 2011; Prsa et al., 2012). To solve the discrepancy

625 between two sensory estimates, the brain may choose to realign all the sensory estimates with respect

626 to the most appropriate one. This interpretation is consistent with the *appropriateness principle* (Welch

627 et al., 1980): discrepancies between senses tend to be resolved in favor of the modality not only

628 generally more reliable, but also more appropriate to the task at hand. Recently, Block and Bastian

629 (2011) demonstrated that the weighting and realigning strategies are two independent processes that

630 might occur in conjunction.

631 In the present experiment, the conflict increase between static and movement information may

632 lead to an apparent suboptimal estimation of the illusion velocity due to a recalibration of the visuo-

633 tactile estimation with respect to the static proprioceptive information. Indeed, the CNS may rely more

634 on less ambiguous information, which is muscle proprioceptive information, rather than on visual or

635 tactile information which can both relate to either self-body or environmental changes. Such a

636 recalibration mechanism could thus explain why the perceptual benefit of the bimodal situation was

637 lower than predicted.

638 To test this hypothesis, we degraded muscle proprioceptive signals in order to reduce the reliability of

639 the static information. Natural messages from muscle spindles were masked thanks to a concomitant

640 vibration applied onto the wrist antagonist muscles (Roll et al., 1989). Such vibration efficiently

641 degraded the information of hand immobility: the velocity required to give rise to an illusory

642 movement with a velocity close to the reference value was lower than previously observed in the

643 *Standard* condition (with no vibration). In other words, the same visual or tactile stimulation gave rise

644 to faster illusory movements when muscle proprioception was masked by the vibration. Using the

645 mirror paradigm, Guerraz et al. (2012) consistently reported that the illusory movement sensation of

646 one arm evoked by the reflection on a mirror of the contralateral moving arm increased with a

647 proprioceptive masking of the arm subjected to kinesthetic illusion.

648 As expected, the proprioceptive noise enabled our model to better fit the observed illusion

649 gains. However, the model predictions still over-estimated the visuo-tactile benefit on gain, suggesting

650 that attenuating muscle proprioceptive feedback was not sufficient. This quantitative discrepancy may

651 be due to incomplete masking of proprioceptive afferents through our non-invasive stimulation. In

652 addition, static information cannot be completely cancelled, since the participants were always aware

26

653 that no actual hand movement was occurring during the experiment. This cognitive component might

654 have pushed towards a sensory realignment in conjunction with a greater muscular proprioception

655 reweighting in the visuo-tactile estimation of illusory hand movements.

656

657 *Physiological evidence for visuo-tactile integration and Bayesian inferences*

658 A large number of studies performed in animals and humans have recently provided compelling

659 evidence for the neural substrates of multisensory integrative processing, including in the early stages of sensory

660 information processing (for reviews see Cappe et al., 2009; Klemen and Chambers, 2012). Bimodal neurons

661 sensitive to both visual and tactile stimuli applied on the hand have been found in the premotor and parietal

662 areas of the monkey (Graziano & Gross, 1998; Grefkes & Fink, 2005), when spatially congruent stimuli from

663 different origins are simultaneously presented to the animal. Neuroimaging studies further support that

664 heteromodal brain regions are specifically activated in the presence of different sensory inputs (Calvert, 2001;

665 Downar et al., 2000; Gentile et al., 2011; Kavounoudias et al., 2008; Macaluso & Driver, 2001). By applying

666 coincident visual and tactile stimuli on human hands, Gentile et al. (2011) used fMRI to show the involvement

667 of the premotor cortex and intraparietal sulcus in visuo-tactile integration processing, supporting observations

668 previously reported in monkeys. More generally, the inferior parietal cortex has been found to subserve visuo-

669 tactile integrative processing for object motion coding in peripersonal space (Bremmer et al., 2001; Grefkes and

670 Fink, 2005) as well as for coding self-body awareness (Kammers et al., 2009; Tsakiris, 2010).

671 Interestingly, direct or indirect interactions between primary sensory areas have been recently evidenced

672 (Ghazanfar & Schroeder, 2006; Cappe et al., 2009). Recently, using an elegant design inspired by the Bayesian

673 framework, Helbig et al. (2012) showed that during a task of shape identification, activation of the primary

674 somatosensory cortex can be modulated by the reliability of visual information within congruent visuo-tactile

675 inputs. The more reliable the visual information, the less activity in S1 increased.

676 Meanwhile, computational modelling approaches have demonstrated that a simple linear summation of neural

677 population activity may account for optimal Bayesian computations (Knill & Pouget, 2004; Ma et al., 2006;

678 Fetsch et al., 2013). By recording single neurones sensitive to both vestibular and visual stimuli within the

679 dorsal medial superior temporal area (MSTd) in monkeys, a brain region activated during self-body motion,

Morgan et al. (2008) provided evidence for the neural basis of Bayesian computations in kinesthesia. During presentation of multisensory stimulation, MSTd neurones displayed responses that were well fit by a weighted linear sum of vestibular and visual unimodal responses.

Altogether these observations support the assumption that the level of activation of primary sensory regions may reflect the relative weight of the sensory cues, and that the perceptual enhancement due to convergent multisensory information might be achieved through a multistage integration processing involving dedicated heteromodal brain regions as well as direct interactions between primary sensory areas. Although the cerebral networks responsible for visuo-tactile integration involved in self-body movement perception remain to be identified, neural recordings from visuo-vestibular cortical regions support the assumption of a Bayesian-like multisensory integration at the cortical level, bridging the gap between neurophysiological, computational and behavioural approaches.

Conclusion

The present findings show for the first time that kinesthetic information from visual and tactile origins is optimally integrated to improve speed discriminative ability for self-hand movement perception. In addition, by inducing illusory movement sensations, we created an artificial conflict between static muscle proprioceptive information and moving tactile and/or visual information. Such sensory conflict might explain the low-perceptual gains of the observed illusions, as attested by the increase in illusion gain when muscle proprioception was masked. However, we observed an over-weighting in favor of the *non-moving hand cues* that cannot be fully predicted by a Bayesian optimal weighting process including a Prior favoring hand immobility. An additional recalibration strategy favoring the less ambiguous information in conflictual situations might explain such bias toward the static proprioceptive cues that are omnipresent and play a crucial rule for kinesthesia.

Acknowledgments

Grants

Disclosures

No conflicts of interest, financial or otherwise, are declared by the authors.

References

Adams WJ, Banks MS, van Ee R. Adaptation to three-dimensional distortions in human vision. *Nat Neurosci* 4: 1063–1064, 2001.

Alais D, Burr D. The Ventriloquist Effect Results from Near-Optimal Bimodal Integration. *Curr Biol* 14: 257–262, 2004.

Bensmaia SJ, Killebrew JH, Craig JC. Influence of visual motion on tactile motion perception. *J Neurophysiol* 96: 1625–1637, 2006.

Blanchard C, Roll R, Roll J-P, Kavounoudias A. Combined contribution of tactile and proprioceptive feedback to hand movement perception. *Brain Res* 1382: 219–229, 2011.

Blanchard C, Roll R, Roll J-P, Kavounoudias A. Differential Contributions of Vision, Touch and Muscle Proprioception to the Coding of Hand Movements. *Plos One* 8: e62475, 2013.

729   **Block HJ, Bastian AJ**. Sensory weighting and realignment: independent compensatory processes. *J*

730   *Neurophysiol* 106: 59–70, 2011.

731   **Brandt T, Dichgans J**. Circular Vection, Visually Induced Pseudocoriolis Effects, Optokinetic Afternystagmus -

732   Comparative Study of Subjective and Objective Optokinetic Aftereffects. *Albrecht Von Graefes Arch*

733   *Klin Exp Ophthalmol* 184: 42–&, 1972.

734   **Bremmer F, Schlack A, Shah NJ, Zafiris O, Kubischik M, Hoffmann KP, Zilles K, Fink GR**. Polymodal motion

735   processing in posterior parietal and promotor cortex: A human fMRI study strongly implies

736   equivalencies between humans and monkeys. *Neuron* 29: 287–296, 2001.

737   **Bresciani J-P, Ernst MO, Drewing K, Bouyer G, Maury V, Kheddar A**. Feeling what you hear: auditory signals

738   can modulate tactile tap perception. *Exp Brain Res* 162: 172–180, 2004.

739   **Breugnot C, Bueno M-A, Renner M, Ribot-Ciscar E, Aimonetti J-M, Roll J-P**. Mechanical Discrimination of Hairy

740   Fabrics from Neurosensorial Criteria. *Text Res J* 76: 835–846, 2006.

741   **Calvert GA**. Crossmodal processing in the human brain: Insights from functional neuroimaging studies. *Cereb*

742   *Cortex* 11: 1110–1123, 2001.

743   **Calvin-Figuière S, Romaiguère P, Gilhodes J-C, Roll J-P**. Antagonist motor responses correlate with kinesthetic

744   illusions induced by tendon vibration. *Exp Brain Res* 124: 342–350, 1999.

745   **Cappe C, Rouiller EM, Barone P**. Multisensory anatomical pathways. *Hear Res* 258: 28–36, 2009.

746   **Clemens IAH, Vrijer MD, Selen LPJ, Gisbergen JAMV, Medendorp WP**. Multisensory Processing in Spatial

747   Orientation: An Inverse Probabilistic Approach. *J Neurosci* 31: 5365–5377, 2011.

748   **van Beers RJ, Wolpert DM, Haggard P.** When Feeling Is More Important Than Seeing in Sensorimotor

749   Adaptation. *Current Biology* 12: 834–837, 2002.

750   **van Dam LC**, **Parise CV**, **Ernst MO**. Modeling Multisensory Integration. *Sensory integration and the unity of*

751   *consciousness*, 2014.

752 **Diener HC, Dichgans J, Guschlbauer B, Mau H.** The significance of proprioception on postural stabilization as

753 assessed by ischemia. *Brain Res* 296: 103-109, 1984.

754 **Dokka K, Kenyon RV, Keshner EA, Kording KP**. Self versus Environment Motion in Postural Control. *Plos*

755 *Comput Biol* 6: e1000680, 2010.

756 **Downar J, Crawley AP, Mikulis DJ, Davis KD**. A multimodal cortical network for the detection of changes in the

757 sensory environment. *Nat Neurosci* 3: 277–283, 2000.

758 **Ernst MO, Banks MS**. Humans integrate visual and haptic information in a statistically optimal fashion. *Nature*

759 415: 429–433, 2002.

760 **Fetsch CR, Turner AH, DeAngelis GC, Angelaki DE**. Dynamic Reweighting of Visual and Vestibular Cues during

761 Self-Motion Perception. *J Neurosci* 29: 15601–15612, 2009.

762 **Fetsch CR, DeAngelis GC, Angelaki DE**. Bridging the gap between theories of sensory cue integration and the

763 physiology of multisensory neurons. *Nat Rev Neurosci* 14: 429–442, 2013.

764 **Gentile G, Petkova VI, Ehrsson HH**. Integration of Visual and Tactile Signals From the Hand in the Human

765 Brain: An fMRI Study. *J Neurophysiol* 105: 910–922, 2011.

766 **Ghazanfar AA, Schroeder CE**. Is neocortex essentially multisensory? *TRENDS COGN SCI* 10: 278–285, 2006.

767 **Gingras G, Rowland BA, Stein BE**. The Differing Impact of Multisensory and Unisensory Integration on

768 Behavior. *J Neurosci* 29: 4897–4902, 2009.

769 **Gori M, Mazzilli G, Sandini G, Burr D**. Cross-sensory facilitation reveals neural interactions between visual and

770 tactile motion in humans. *Percept Sci* 2: 55, 2011.

771 **Graziano MSA, Gross CG**. Spatial maps for the control of movement. *Curr Opin Neurobiol* 8: 195–201, 1998.

772 **Grefkes C, Fink GR**. The functional organization of the intraparietal sulcus in humans and monkeys. *J Anat* 207:

773 3–17, 2005.

774   **Guerraz M, Bronstein AM**. Mechanisms underlying visually induced body sway. *Neurosci Lett* 443: 12–16,

775   2008.

776   **Guerraz M, Provost S, Narison R, Brugnon A, Virolle S, Bresciani J-P**. Integration of visual and proprioceptive

777   afferents in kinesthesia. *Neuroscience* 223: 258–268, 2012.

778   **Helbig HB, Ernst MO, Ricciardi E, Pietrini P, Thielscher A, Mayer KM, Schultz J, Noppeney U**. The neural

779   mechanisms of reliability weighted integration of shape information from vision and touch.

780   *Neuroimage* 60: 1063–1072, 2012.

781   **Jürgens R, Becker W**. Perception of angular displacement without landmarks: evidence for Bayesian fusion of

782   vestibular, optokinetic, podokinesthetic, and cognitive information. *Exp Brain Res* 174: 528–543, 2006.

783   **Kammers MPM, Verhagen L, Dijkerman HC, Hogendoorn H, De Vignemont F, Schutter DJLG**. Is This Hand for

784   Real? Attenuation of the Rubber Hand Illusion by Transcranial Magnetic Stimulation over the Inferior

785   Parietal Lobule. *J Cogn Neurosci* 21: 1311–1320, 2009.

786   **Kavounoudias A, Roll JP, Anton JL, Nazarian B, Roth M, Roll R**. Proprio-tactile integration for kinesthetic

787   perception: An fMRI study. *Neuropsychologia* 46: 567–575, 2008.

788   **Klemen J, Chambers CD**. Current perspectives and methods in studying neural mechanisms of multisensory

789   interactions. *Neurosci Biobehav Rev* 36: 111–133, 2012.

790   **Knill DC, Pouget A**. The Bayesian brain: the role of uncertainty in neural coding and computation. *Trends in*

791   *Neurosciences* 27: 712–719, 2004.

792   **Körding KP, Beierholm U, Ma WJ, Quartz S, Tenenbaum JB, Shams L.** Causal Inference in Multisensory

793   Perception. PLoS ONE 2: e943, 2007.

794   **Landy MS, Banks MS, Knill DC**. Ideal-Observer Models of Cue Integration. In: *Sensory Cue Integration*. 2011.

795   **Laurens J, Droulez J**. Bayesian processing of vestibular information. *Biol Cybern* 96: 389–404, 2006.

796 **Ma WJ, Beck JM, Latham PE, Pouget A**. Bayesian inference with probabilistic population codes. *Nat Neurosci*

797   9: 1432–1438, 2006.

798 **Macaluso E, Frith C, Driver J**. Multisensory integration and crossmodal attention effects in the human brain -

799   Response. *Science* 292, 2001.

800 **McCloskey D**. Kinesthetic Sensibility. *Physiol Rev* 58: 763–820, 1978.

801 **Montagnini A, Mamassian P, Perrinet L, Castet E, Masson GS**. Bayesian modeling of dynamic motion

802   integration. *J Physiol-Paris* 101: 64–77, 2007.

803 **Morgan ML, DeAngelis GC, Angelaki DE**. Multisensory integration in macaque visual cortex depends on cue

804   reliability. *Neuron* 59: 662–673, 2008.

805 **Proske U, Gandevia SC**. The Proprioceptive Senses: Their Roles in Signaling Body Shape, Body Position and

806   Movement, and Muscle Force. *Physiol Rev* 92: 1651–1697, 2012.

807 **Prsa M, Gale S, Blanke O**. Self-motion leads to mandatory cue fusion across sensory modalities. *J Neurophysiol*

808   108: 2282–2291, 2012.

809 **Reuschel J, Drewing K, Henriques DYP, Rösler F, Fiehler K**. Optimal integration of visual and proprioceptive

810   movement information for the perception of trajectory geometry. *Exp Brain Res* 201: 853–862, 2009.

811 **Roach NW, Heron J, McGraw PV**. Resolving multisensory conflict: a strategy for balancing the costs and

812   benefits of audio-visual integration. *Proc R Soc Lond B Biol Sci* 273: 2159–2168, 2006.

813 **Roll J, Vedel J, Ribot E**. Alteration of Proprioceptive Messages Induced by Tendon Vibration in Man - a

814   Microneurographic Study. *Exp Brain Res* 76: 213–222, 1989.

815 **Roll J, Gilhodes J, Roll R, Velay J**. Contribution of Skeletal and Extraocular Proprioception to Kinesthetic

816   Representation. *Atten Perform* : 549–566, 1990.

817 **Sober SJ, Sabes PN.** Multisensory integration during motor planning. *J Neurosci 23*: 6982–6992, 2003.

818   **Sober SJ, Sabes PN**. Flexible strategies for sensory integration during motor planning. *Nat Neurosci* 8: 490–

819   497, 2005.

820   **Stein BE, Stanford TR, Ramachandran R, Perrault TJ, Rowland BA**. Challenges in quantifying multisensory

821   integration: alternative criteria, models, and inverse effectiveness. *Exp Brain Res* 198: 113–126, 2009.

822   **Stocker AA, Simoncelli EP**. Noise characteristics and prior expectations in human visual speed perception. *Nat*

823   *Neurosci* 9: 578–585, 2006.

824   **Tagliabue M, McIntyre J**. When Kinesthesia Becomes Visual: A Theoretical Justification for Executing Motor

825   Tasks in Visual Space. *PLoS ONE* 8: e68438, 2013.

826   **Tsakiris M**. My body in the brain: A neurocognitive model of body-ownership. *Neuropsychologia* 48: 703–712,

827   2010.

828   **Vidal M, Bülthoff HH**. Storing upright turns: how visual and vestibular cues interact during the encoding and

829   recalling process. *Exp Brain Res* 200: 37–49, 2009.

830   **Weiss Y, Simoncelli EP, Adelson EH**. Motion illusions as optimal percepts. *Nat Neurosci* 5: 598–604, 2002.

831   **Welch R, Warren D, With R, Wait J**. Visual capture - the effects of compellingness and the assumption of unity.

832   *Bull Psychon Soc* 16: 168–168, 1980.

833   **Wichmann FA, Hill NJ**. The psychometric function: II. Bootstrap-based confidence intervals and sampling.

834   *Percept Psychophys* 63: 1314–1329, 2001.

835   **Wozny DR, Beierholm UR, Shams L**. Human trimodal perception follows optimal statistical inference. *J Vis* 8:

836   24, 2008.

837   **Wozny DR, Shams L**. Computational characterization of visually induced auditory spatial adaptation. *Front*

838   *Integr Neurosci* 5: 75, 2011.

Figure Captions

840

841   **Figure 1: Experimental set-up and stimulation devices**

842   A: Experimental set-up including stimulation devices and motion capture system (CODAmotion) to

843   record actual right hand movements in the reference movement condition. B: Textured-disk used as

844   tactile stimulation. C: Visual pattern displayed by a video projector (see A). D: Mechanical vibrators

845   applied onto two antagonist wrist muscles (*pollicis longus* and *extensor carpi ulnaris*) to disturb

846   muscle proprioceptive inputs (MP) in the *Noisy* condition

847   Participants exposed to a counterclockwise rotation of the tactile and/or visual stimuli had to report

848   whether the induced clockwise illusion of hand rotation they perceived was faster or slower than the

849   velocity of the reference movement they actively executed before or after each stimulation.

850

851   **Figure 2: Schematic representation of the MLE principle**

852   In order to estimate self-hand movement velocity, the CNS is supposed to proceed as an inference

853   machine: following MLE rules, unisensory cues (noisy, normally-distributed representations of the

854   stimulation velocity ϑ_T and ϑ_V on the basis of each sensory modality, touch and vision) are optimally

855   combined to determine the minimum-variance visuo-tactile perceptual estimate ϑ_{VT}. The right panel

856   illustrates the MLE prediction for the visuo-tactile Likelihood (with variance σ^2_{VT}, black curve)

857   resulting from the optimal combination of unimodal Likelihoods (σ^2_T, σ^2_V, dark grey and light grey

858   curves, respectively).

859

860   **Figure 3: Relationship between Bayesian and psychometric functions**

861   A and B represent two different relevant conditions of stimulations (1 and 2) used to determine the

862   discriminative threshold: the PSE (A) and the intensity leading to 84.13 % of "faster than the reference

863   velocity" answer (B). V_{ref} is the velocity of the reference movement (5 °/s). σ_{Post}, μ_{Post} and μ_i are

parameters of the Bayesian functions, respectively the standard deviation and mean of the Posterior

distribution and the mean of the Likelihood function (assumed equal to the stimulation velocity). σ_Ψ

and PSE are the psychophysical, measured parameters, respectively the variance and the mean of the

psychometric function. We remind that the PSE is defined as the point of subjective equality, i.e. the

stimulation intensity eliciting an illusory movement faster than the reference 50 % of the time. These

relations allow to estimate all the parameters of the hidden Bayesian functions as a function of the

psychometric parameters (see in Models).

Figure 4: Schematic representation of the key steps for predicting visuo-tactile gain on the basis of a Prior-equipped Bayesian model.

Step 1: Prior variability estimation: the standard deviation (σ_{Prior}) of the Prior distribution (black curve, centered on the null velocity) is estimated for each participant using (through Equation 6) the psychometric parameters estimated in unimodal visual (orange curves) and tactile (blue curves) conditions.

Step 2: Prediction of visuo-tactile gain: the expected PSE (Point of subjective equality) in visuo-tactile stimulation (mean of the visuo-tactile Likelihood depicted by the dashed green curve) is predicted on the basis of the estimate of the Prior variance (step 1), the MLE-estimate for σ^2_{VT} and Equation 7. The visuo-tactile gain is simply derived from the PSE (see definition in Method).

Figure 5: Comparison of velocity discrimination thresholds during tactile, visual and visuo-tactile stimulation

A. Extraction of σ from psychometric curves: Psychometric curves of one representative participant obtained by fitting the probabilities of perceiving the illusion as faster than the reference movement with a cumulative Gaussian distribution for the tactile stimulation (T, blue curve), visual stimulation

888 (V, yellow curve), and visuo-tactile stimulation (VT, green curve). The discrimination threshold, σ, is

889 the difference between the stimulation velocities leading to the «faster» answer 84.13 % of the times

890 and 50 % of the times, and it is inversely related to the slope of the psychometric function.

891 **B. Mean σ in bi- or unimodal stimulation**: Mean individual values of σ (grey bars) and mean (± SD)

892 values of σ extracted from the whole population data (N = 15) for tactile (blue square), visual (yellow

893 square), and visuo-tactile (green square) stimulation. For the mean σ values, significant differences

894 were found between the bimodal and each of the two unimodal conditions (* $P < .05$; ** $P < .01$).

895 **C. Multisensory Index for σ**: individual (grey bars) and mean Multisensory Index (MSI; green

896 square) for σ (N = 15 participants). Positive and negative values correspond respectively to a

897 multisensory benefit or loss in the discrimination performance of the participants with respect to their

898 most efficient unimodal performance.

899 **D. Comparison between observed and MLE-predicted σ**: Comparison between observed σ in visuo-

900 tactile stimulation and σ predicted by the MLE model for the 15 participants (S1 to S15). The green

901 diamonds correspond to the observed data and the error bars are the standard deviation. No significant

902 difference was found between predictions and observations of σ ($P = .55$, ns). Light green rectangles

903 represent 95 % CIs computed using the following bootstrap procedure. Choice data were resampled

904 across repetitions (with replacement) and refitted 1000 times to create sample-distributions of the

905 threshold for each psychometric function and for the predicted visuo-tactile parameters. The CIs were

906 directly estimated from these bootstrap-samples (percentile method).

907

908 **Figure 6: Comparison of the gains of the perceptual responses during tactile, visual and**

909 **visuo-tactile stimulation**

910 **A. Extraction of PSE from psychometric curves**: Psychometric curves of one participant obtained

911 by fitting the probability of perceiving the illusion as "faster than the reference" movement with a

cumulative Gaussian distribution for the tactile stimulation (T, blue curve), visual stimulation (V, yellow curve), and visuo-tactile stimulation (VT, green curve). The PSE (Point of Subjective Equality) corresponds to the stimulation velocity leading to the «faster than the reference» answer 50 % of the time.

B. Mean Gain in bi- or unimodal stimulation: Mean individual values of gain (grey bars) and mean (± SD) values of gain calculated as the ratio between the reference velocity, V_{ref}, and the actual velocity of the visual (yellow bars), tactile (blue bars) and visuo-tactile (green bars) stimulation at the PSE. For the mean gain values, significant differences were found between the bimodal and each of the two unimodal conditions (* $P < .05$; ** $P < .01$).

C. Multisensory Index for Gain: Individual (grey bars) and mean Multisensory Index (MSI; green square) of illusion gains (N=15 participants). Positive and negative values correspond respectively to a multisensory increase or decrease in the gain of the perceptual illusions of the participants with respect to the best unimodal performance.

D. Comparison between observed and Bayesian predicted Gain: Comparison between observed gain in visuo-tactile stimulation and gain predicted by the Bayesian model with a zero-centered Prior for the 15 participants (S1 to S15). The green diamonds correspond to the observed data and the error bars are the standard deviation. The increase of the bimodal gain was predicted but over-estimated by the model. Light green rectangles represent 95 % CIs computed using the following bootstrap procedure. Choice data were resampled across repetitions (with replacement) and refitted 1000 times to create sample-distributions of the threshold for each psychometric function and for the predicted visuo-tactile parameters. The CIs were directly estimated from these bootstrap-samples (percentile method).

Figure 7: Comparison of illusion gains between *Standard* and *Noisy* conditions

Mean gain (± SEM) of the discrimination responses induced by tactile (T, squares), visuo-tactile (VT, triangles), and visual (V, diamonds) stimulation for the *Standard* (plain grey) and the *Noisy* (hatched grey) conditions. Note that illusion gains observed in the *Noisy* conditions, in which muscle proprioception afferents were masked by an ago-antagonist co-vibration, were significantly higher than those in the *Standard* conditions whatever the stimulation (T, V, VT). * $P < .05$; ** $P < .01$

Figure 8: Comparison of the Bayesian predictions for the *Standard* and *Noisy* conditions

A. Bayesian prediction vs observation in Noisy condition: Comparison between observed gains in visuo-tactile stimulation and gains predicted by the Bayesian model in the <u>*Noisy*</u> condition for the 13 participants (S1 to S13). The dots correspond to individual observed data and the error bars are the standard deviation. represent 95 % CIs computed using the following bootstrap procedure. Choice data were resampled across repetitions (with replacement) and refitted 1000 times to create sample-distributions of the threshold for each psychometric function and for the predicted visuo-tactile parameters. The CIs were directly estimated from these bootstrap-samples (percentile method). Increase of the visuo-tactile gain was better predicted than in the *Standard* condition but remained over-estimated by the model.

B. Difference between prediction and observation Gain$_{pred}$ - Gain$_{obs}$: The quantitative difference between model predictions and empirically obtained values of visuo-tactile gain was significantly smaller in the *Noisy* condition compared to the *Standard* condition ($P < .05$).
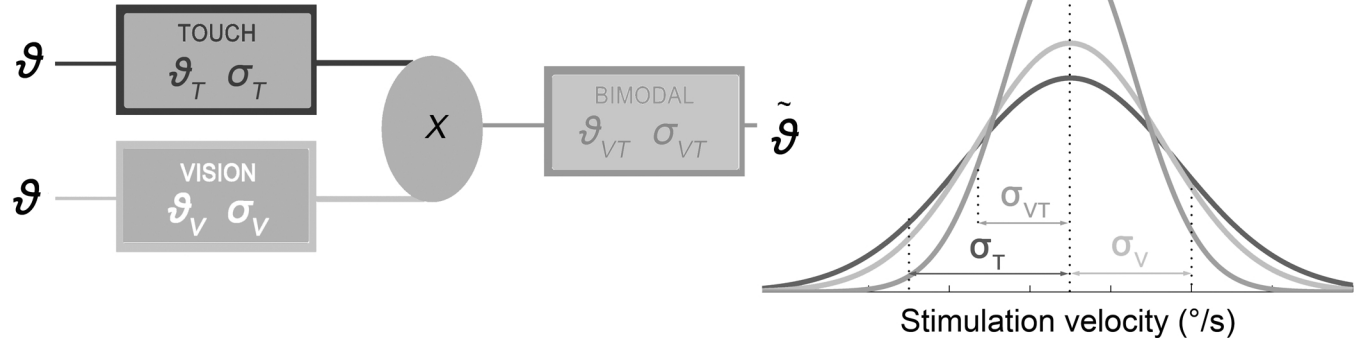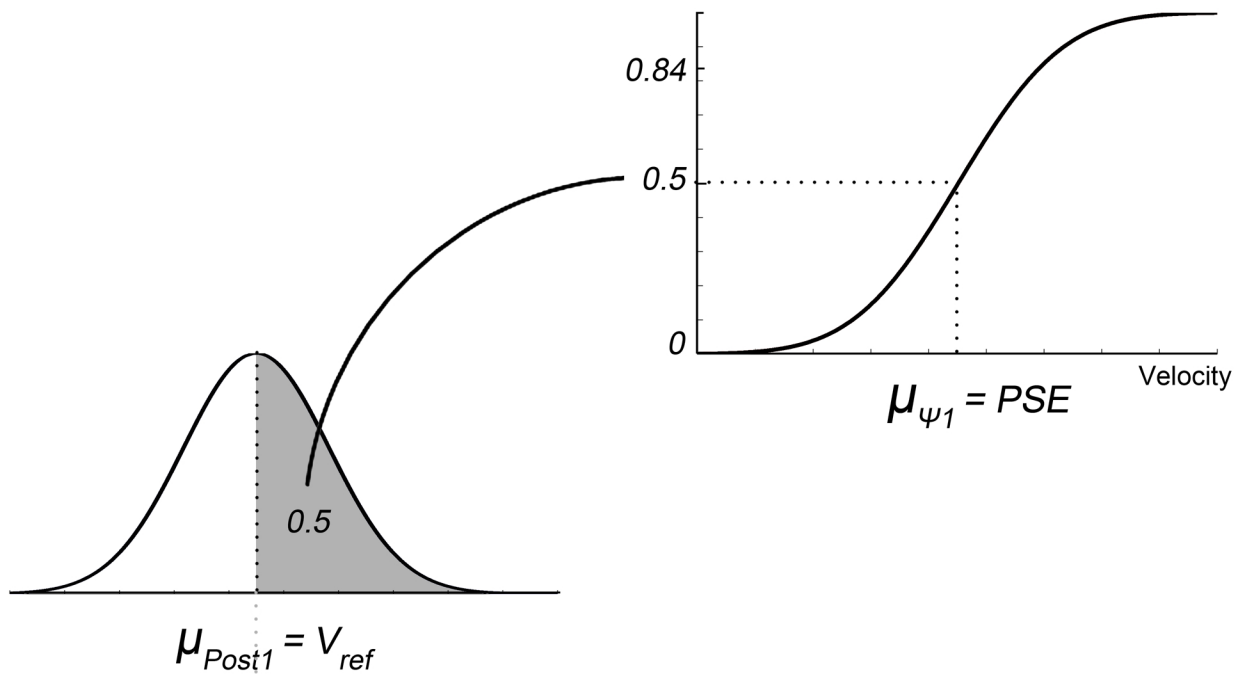
A.
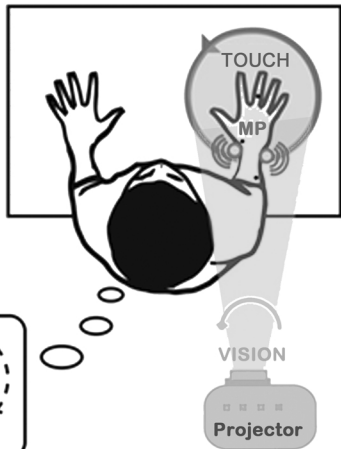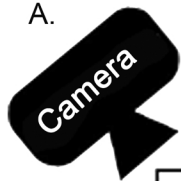
B.
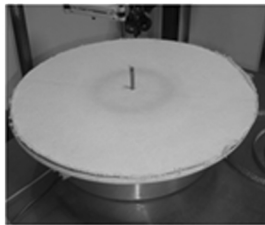
C.
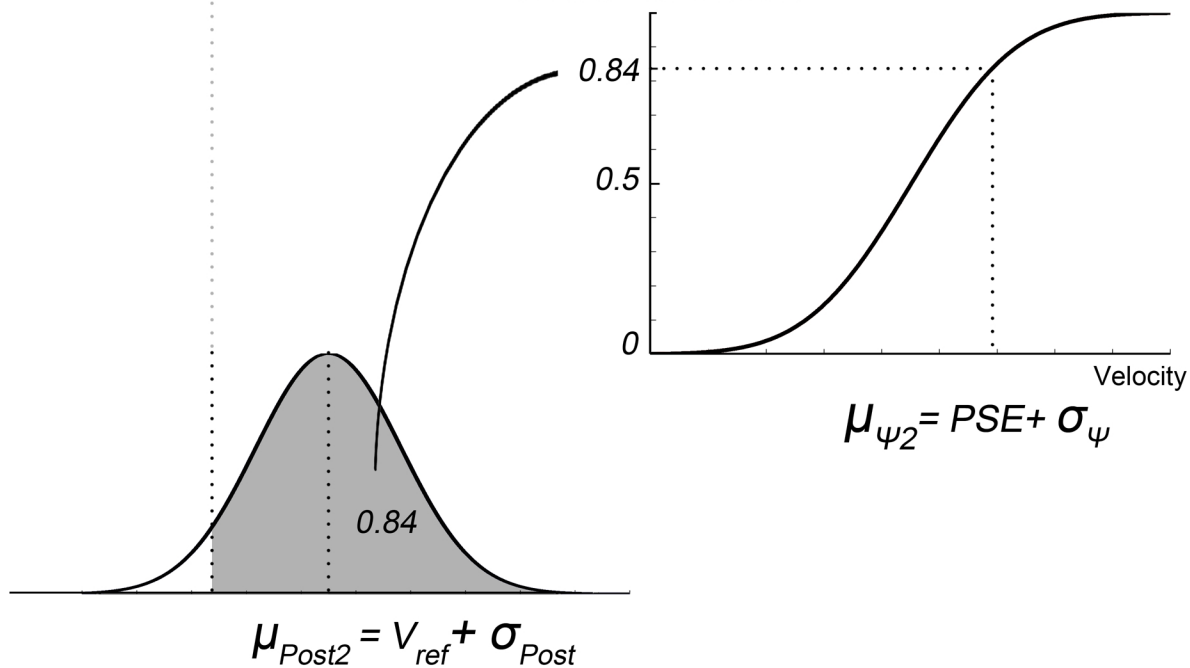
D.

MLE principle

Stimulation velocity (°/s)

A

Proportion of answers
«test faster than reference»

0.84

0.5

0

Velocity

$\mu_{\psi 1} = PSE$

0.5

$\mu_{Post1} = V_{ref}$

B

Proportion of answers
«test faster than reference»

0.84

0.5

0

Velocity

$\mu_{\psi 2} = PSE + \sigma_{\psi}$

0.84

$\mu_{Post2} = V_{ref} + \sigma_{Post}$

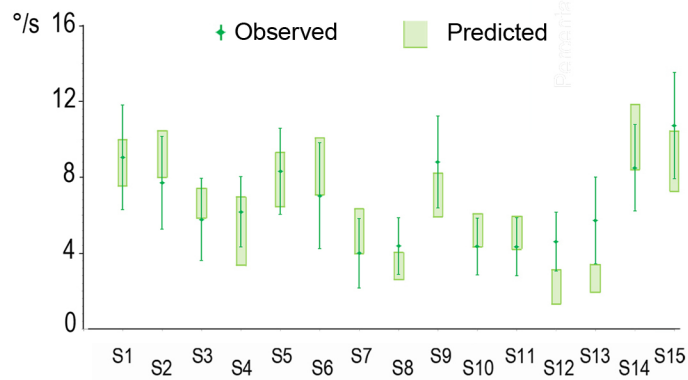**A** σ extraction from psychometric curves

B Mean σ under bi- or unimodal stimulation

C Multisensory index for σ

D Observed and MLE-predicted σ

A (y-axis) Percentage of «faster» answers — 84%, 50% — (x-axis) Velocity (°/s) — 10, 25, 45 — σ_{VT}, σ_T, σ_V

B °/s — 16, 12, 8, 4, 0 — σ_T, σ_{VT}, σ_V — **

C 40%, 0%, -40% — Benefit

D °/s — 16, 12, 8, 4 — Observed, Predicted — S1 S2 S3 S4 S5 S6 S7 S8 S9 S10 S11 S12 S13 S14 S15

A PSE extraction from psychometric curves

Percentage of «faster» answers

100%

50%

10   25   45
Velocity (°/s)

PSE$_{VT}$
PSE$_V$
PSE$_T$
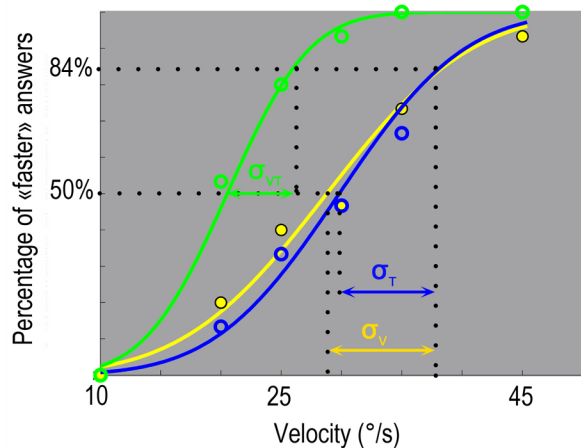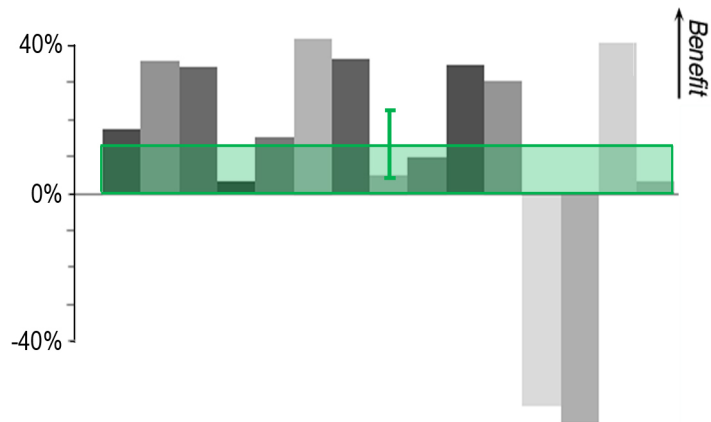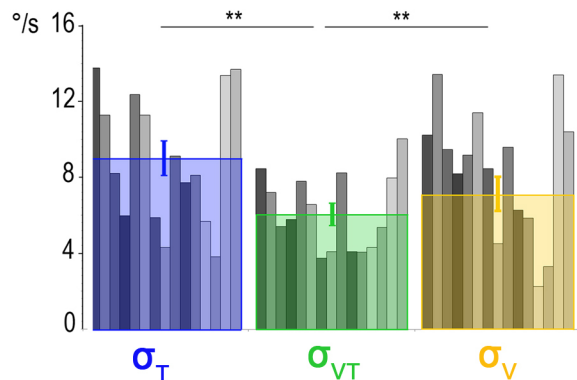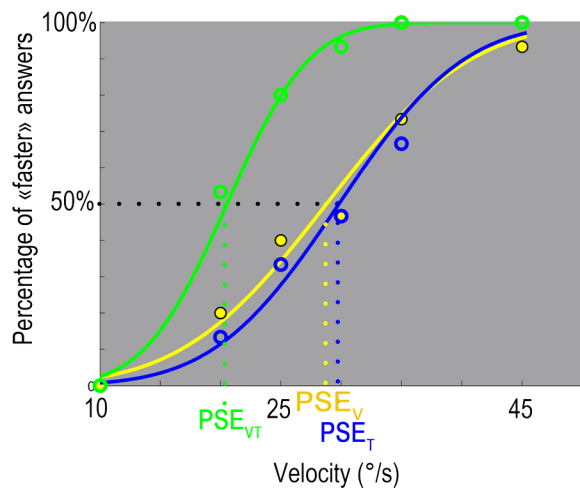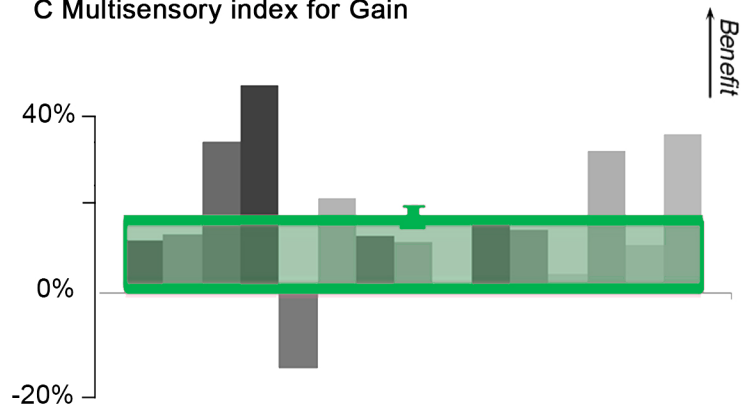
B Mean Gain under bi- or unimodal stimulation

40%

20%

0%

** **

Gain$_T$ Gain$_{VT}$ Gain$_V$

C Multisensory index for Gain

Benefit

40%

0%

-20%

D Observed and Bayesian predicted Gain

+ Observed   Predicted

40%

20%

0%

S1 S2 S3 S4 S5 S6 S7 S8 S9 S10 S11 S12 S13 S14 S15

A

B